IN-SITU CREEP TESTING CAPABILITY FOR THE ADVANCED TEST REACTOR

MATERIALS FOR NUCLEAR SYSTEMS

KEYWORDS: *creep testing, Advanced Test Reactor, pressurized water reactor conditions*

BONG GOO KIM,[a]* JOY L. REMPE,[b] DARRELL L. KNUDSON,[b] KEITH G. CONDIE,[b] and BULENT H. SENCER[b]

[a]*Korea Atomic Energy Research Institute, 989-111 Daedeok-daero Yuseong-gu, Daejeon 305-600, Korea*
[b]*Idaho National Laboratory, P.O. Box 1625, MS 3840, Idaho Falls, Idaho 83415*

Received April 1, 2010
Accepted for Publication October 24, 2011

An instrumented creep testing capability is being developed for specimens irradiated in pressurized water reactor coolant conditions at the Advanced Test Reactor (ATR). A test rig has been developed such that samples will be subjected to stresses up to 350 MPa at temperatures up to 370°C in pile. Initial Idaho National Laboratory (INL) efforts to develop this creep testing capability for the ATR are summarized. In addition to providing an overview of in-pile creep test capabilities available at other test reactors, this paper reports efforts by the INL to evaluate a prototype test rig in an autoclave at INL's High Temperature Test Laboratory. Data from autoclave tests with Type 304 stainless steel and copper specimens are reported.

I. INTRODUCTION

Irradiation creep is the additional strain that occurs as a result of the combined effect of irradiation and stress in materials. The strain occurring in the absence of irradiation is generally called thermal creep. Performance of fuel, cladding, reactor pressure vessels, and other core components of nuclear power reactors can be affected by dimensional instabilities caused by creep. Hence, it is necessary to assess the amount of creep expected to occur for a component during its service time in a reactor. Irradiation creep of materials, in particular stainless steel, is an important concern for structures subjected to irradiation in fast breeder and fusion reactors.[1–8] In addition, the study of irradiation creep is important in assessing the ability of core structural materials to survive extended lifetimes in light water reactors (LWRs).

Often, irradiation creep is measured using a "cook-and-look" approach where samples are irradiated for a period of time, removed from the reactor, measured, and then returned to the reactor. Repetition of this process can be expensive and time consuming. It is therefore desirable to obtain in-pile measurements of creep samples during irradiation. As part of the Advanced Test Reactor (ATR) National Scientific User Facility (NSUF), efforts were initiated to develop an instrumented creep testing capability for specimens irradiated in pressurized water reactor (PWR) coolant conditions at the ATR. A creep test rig was developed such that samples will be subjected to applied loads up to 350 MPa at temperatures as high as 370°C in pile. This paper summarizes the status of Idaho National Laboratory (INL) efforts to develop an in-pile creep testing capability for the ATR. In addition to providing an overview of in-pile creep test capabilities available at other test reactors, this paper describes efforts to evaluate a prototype test rig in an autoclave at INL's High Temperature Test Laboratory (HTTL). Comparison stainless steel data are also summarized and are used for evaluating initial results from these autoclave tests. Additional details about this effort may be found in Ref. 9.

*E-mail: bgkim1@kaeri.re.kr

II. BACKGROUND

II.A. Fundamentals

Creep is a slow and time-dependent strain that occurs in a material subjected to a stress (or load) at relatively high temperatures. A typical creep curve is shown

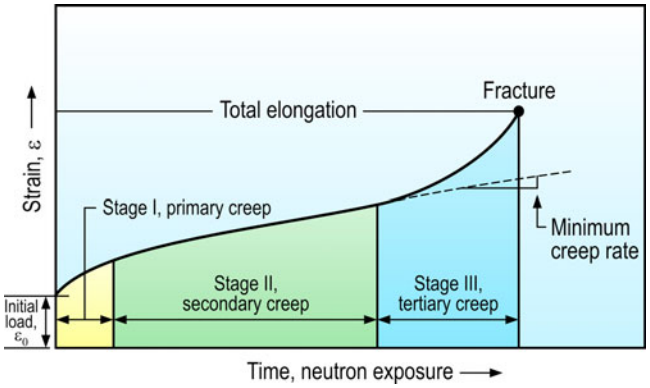

Fig. 1. Representative creep curve.

in Fig. 1. In a creep test, a constant load is applied to a tensile specimen generally maintained at a constant temperature. Strain is then measured over time. Primary creep, or stage I creep, is associated with the time during which the creep rate decreases due to work hardening of the material. During this stage, initial hardening takes place and the resistance to creep increases until stage II, or secondary, creep begins. Secondary creep is associated with the time during which the creep rate is roughly constant. Stage II is referred to as steady-state creep because a balance is achieved between the work hardening and annealing (thermal softening) processes. The slope of the curve during stage II creep is the strain rate or the creep rate of the material. Tertiary creep, or stage III creep, occurs when there is a reduction in cross-sectional area due to necking or an effective reduction in area due to internal void formation. The creep rate increases due to necking of the specimen and the associated increase in local stress. If stage III creep is allowed to continue, specimen fracture will occur.

Creep data are generally analyzed in terms of three variables: time, stress, and temperature. Most uniaxial creep is conducted under constant load and/or constant temperature conditions. Although the method is simple, the stress in the gauge length of the specimen varies with time. This can be seen clearly by considering a specimen of length L_o and cross-sectional area A_o subjected to a tensile load P. At time $t = 0$, the initial engineering stress σ_o on the specimen is

$$\sigma_o = P/A_o \ . \tag{1}$$

With the assumption of uniform deformation during creep, the specimen lengthens to L, and the cross-sectional area decreases to A, because volume must be conserved. Hence,

$$LA = L_o A_o \ . \tag{2}$$

Therefore,

$$A = A_o(L_o/L) \ , \tag{3}$$

and the true stress σ on the specimen is

$$\sigma = P/A = \sigma_o(L/L_o) \ . \tag{4}$$

II.B. Existing In-Pile Evaluations

During the past 50 years, a large number of tests have been performed to analyze the degradation of mechanical properties as a function of fluence and temperature. Results from these tests are used to assess the safety and lifetime of materials used in structural components of operating nuclear power plants (NPPs). Recently, it is increasingly emphasized that research on neutron irradiation effects of materials is also necessary in order to assess the integrity and lifetime extension of operating NPPs and to develop fuels and materials supporting advanced reactor systems. During irradiation tests in materials test reactors (MTRs), it is desirable to measure characteristic changes in mechanical properties. In particular, efforts are currently emphasizing methods to measure dimensional changes (elongation) of materials during creep tests in MTRs.

There are two types of creep tests completed in MTRs. The first are instrumented tests with online monitoring and control of test conditions and real-time detection of creep rate. The second are noninstrumented cook-and-look tests with specimen evaluation completed outside the reactor and test parameters derived from reactor operating conditions. In instrumented experiments, parameters such as specimen temperature, the load exerted on the specimen, and specimen elongation are monitored and/or controlled using suitable components [extensometers, linear variable differential transformers (LVDTs), bellows, optical transducers, thermocouples, small heaters, etc.] that are positioned in proximity to the specimen under investigation. Instrument selection must consider radiation effects on sensor performance. Such instrumented experiments are complicated to design and are expensive to conduct. Furthermore, there are limited test positions and space available in MTRs for such instrumented tests. Noninstrumented experiments are comparatively simple in design, enable larger numbers of specimens to be tested at a time, and are less expensive to complete. However, irradiation creep using noninstrumented devices must be measured using a cook-and-look approach where samples are irradiated in pile for a time, removed from the reactor, measured outside the reactor, and then returned to the reactor. Repetition of this process can be expensive and time consuming and has the potential to disturb the phenomena of interest. Creep tests with in-pile measurement of specimen elongation under irradiation are able to offer more detailed information of creep behavior of the material. Therefore, instrumented experiments offer more control over experimental variables and improved data accuracy than possible with a "cook-and-look" approach in noninstrumented experiments.

As indicated in Table I, several countries are conducting in-pile creep tests that can provide real-time data related to specimen elongation and controlled loads applied to the specimens.[2,9–25] However, most of the existing and planned tests are conducted in inert gas. The only tests conducted in reactor coolant were completed at the BR2 reactor in Mol, Belgium.

Uniaxial tensile tests for specimens irradiated in reactor coolant at a constant strain rate were performed in the BR2 reactor.[10,11] The purpose of the work was to design, construct, and calibrate a tensile loading module for instrumented tensile tests in the BR2. The actual test rig with this module was developed as shown in Fig. 2. The materials used in this test were thin (0.3-mm) sheets of oxygen-free high-conductivity (OFHC) copper and CuCrZr alloy. The tensile modules, together with tensile test specimen, were irradiated with a neutron flux of 3×10^{17} $nm^{-2}s^{-1}$ ($E > 1$ MeV), corresponding to $\sim 6 \times 10^{-8}$ displacements per atom (dpa)/s. The temperature of the test module increased rapidly due to gamma heating power of 4.4 W/g, and the stagnant reactor pool water close to the test specimen reached an equilibrium temperature of ~90°C within ~10 to 15 min. No load was applied to the tensile specimen during this initial period, but elongation in the specimen was monitored with an LVDT. The uniaxial tensile test, using a constant strain rate of 1.3×10^{-7}/s, was started about 4 h after the rig was inserted in the reactor core. Figure 3 shows a representative stress-strain curve obtained during in-reactor tensile tests for pure (OFHC) copper specimens. Results from this effort suggest that it is technically feasible to carry out well-defined, controlled-load, dynamic tensile tests in pile.

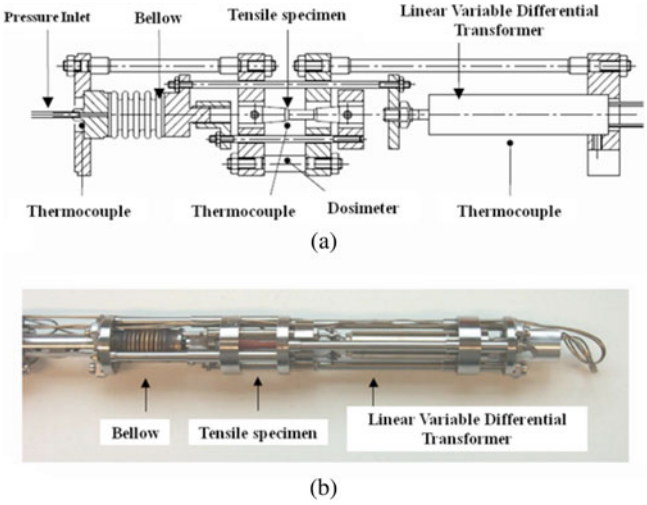

Fig. 2. Tensile test rig for BR2 irradiations: (a) simplified layout illustrating operational features and instrumentation and (b) final assembly of test module prior to installation in the test rig.[10,11]

TABLE I
Summary of Creep Testing in MTRs

Country and Reactor	Test Conditions	Real-Time Load Control	Method	Real-Time Elongation Detection	Method
Belgium, BR2	Stagnant reactor coolant (~90°C)	Yes	Internally pressurized bellows	Yes	Monitored LDVT
France, OSIRIS[a]	Inert gas, water, and NaK (from room temperature up to 380°C)	Yes	Internally pressurized bellows	Yes	Monitored LDVT; external diameter gauges also used
Norway, HBWR	Inert gas (240°C to 400°C)	Yes	Internally pressurized bellows	Yes	Monitored LVDT; external diameter gauges also to be used (under development for 600°C and 250 bar)
Japan, JMTR	Inert gas (550°C)	Yes	Internally pressurized bellows	Yes	Monitored LVDT
Netherlands, HFR	Inert gas and NaK (300°C to 600°C)	Yes	Self-contained spring washer system	Yes (semicontinuous)	Monitored LVDT
Korea, HANARO	Inert gas (up to 600°C)	Yes	Internally pressurized bellows	Yes	Monitored LDVT

[a]In upcoming tests. Previous tests relied on out-of-pile measurements with strain gauges.

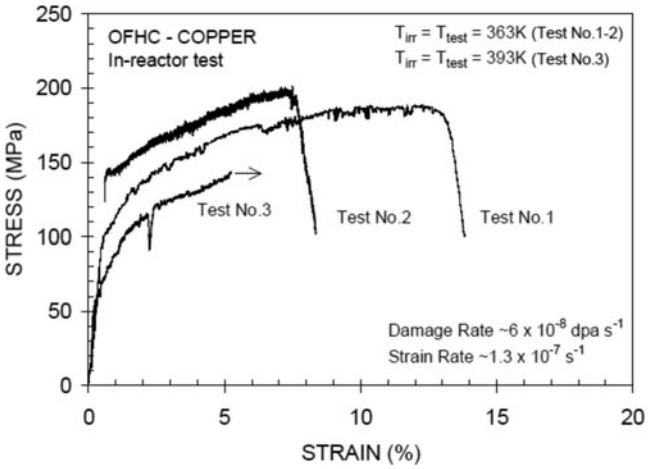

Fig. 3. Representative stress-strain curves of OFHC copper tested in the BR2 reactor at test temperatures of 363 and 393 K (Ref. 10).

Figure 4 shows the conceptual design and representative components of an irradiation creep capsule for testing in inert gas at the HANARO reactor in the Republic of Korea.[22–25] The capsule contains four tensile specimens for an irradiation creep test in inert gas. The Type 316L stainless steel tensile specimens were 1.8 mm in diameter and 30 mm in gauge length. The objective of this test was not only to confirm the design of the creep capsule, but also to compare the performance of an LVDT made by the Institute for Energy Technology/Halden Reactor Project (IFE/HRP) and a commercial vendor. The irradiation creep capsule was designed to expose specimens to temperatures up to 600°C and stresses up to 253 MPa.

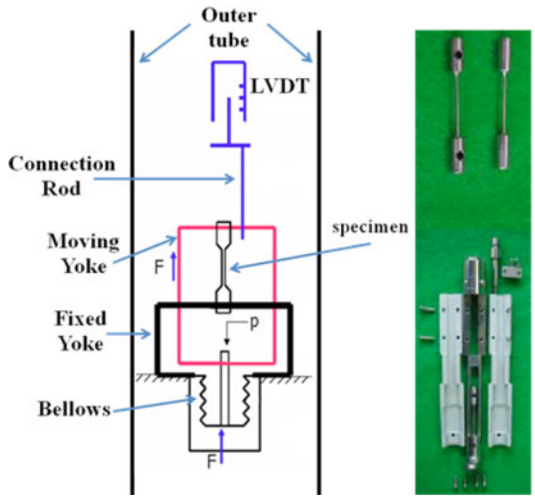

Fig. 4. Conceptual design and selected parts of HANARO irradiation creep capsule prior to assembly.[22–25]

Note that key components in the BR2 and the proposed HANARO test rigs are similar. Each design contains a tensile specimen, a bellows for applying a load to the specimen, an LVDT to detect specimen elongation, and thermocouples to monitor specimen temperature. In both designs, gas is supplied to the bellows internally to control the load applied to the specimen. Cables extending from the LVDT and thermocouples allow specimen temperature and elongation to be monitored during irradiation.

II.C. Existing Type 304 Stainless Steel Data

Although the INL-developed creep testing capability will ultimately be used for a wide range of materials, initial efforts focused on Type 304 stainless steel. As an initial step in this effort, Type 304 stainless steel data found in the literature were reviewed to gain insights about the effects of temperature and radiation on its structural properties.

Table II summarizes sources for Type 304 stainless steel found in the literature.[26–34] As indicated in Table II, Young's modulus (YM), yield strength (YS), and tensile strength (TS) values of stainless steels exhibit a strong dependence on various product forms and/or manufacturing histories (e.g., cold working, hot working, or annealing, etc.). Figures 5, 6, and 7 compare available data for Young's modulus, yield strength, and tensile strength of Type 304 stainless steels.

Figure 5 compares Type 304 stainless steel yield strength and tensile strength data from Refs. 29 through 32. INL data[29] were obtained from specimens fabricated from round bar that was annealed for 1 h at 1323 K and forced-air cooled prior to testing. The American Society of Mechanical Engineers (ASME) codes for various Type 304 stainless steel product forms and/or manufacturing histories are minimum values recommended by ASME; these ASME strengths are averaged values presented in Ref. 30. As indicated in Fig. 5, all of the references indicate that these alloys exhibit strong temperature dependencies of yield strength and tensile strength where the strengths decrease as the test temperature increases.

Figure 6 shows Young's modulus of stainless steels as a function of temperature.[29,31–33] In Fig. 6, the line indicates Young's modulus for typical stainless steels, such as Types 304, 310, 316, 321, and 347. There is also considerable scatter in the Young's modulus data shown in Fig. 6. This is attributed to differences in test uncertainties and material composition. Figure 7 compares selected engineering stress-strain curves for Type 304 stainless steels: typical Type 304 stainless steel,[28] Type 304 stainless steel annealed at 1050°C for 30 min after machining,[32] and Type 304 stainless steel hot rolled by solution heat treatment at 1150°C for 1 h before machining.[31] Curves in this plot illustrate that Type 304 stainless steel strength decreases as temperature increases. However, the large variations in stress-strain curves suggest

TABLE II

Summary of Stainless Steel Data Found in the Literature

Source	Materials (Stainless Steel)	Cold Worked/Annealed	Hot Worked/Annealed	Annealed	Test Temperature Range	YM (GPa)	YS (MPa)	TS (MPa)
Atlas Steels[26] and Touloukian et al.[27]	304, 304H, 316 304L, 316L			✓ ✓	RT[a] RT	193 193	205 170	515 485
Metals Handbook Vol. 3, *Properties and Selection*[28]	304, 316	 ✓	✓		RT RT		205 310	515 620
	304L, 316L	 ✓	✓		RT RT	170	480 310	 620
	304N, 316N			✓	RT		240	550
	304LN, 316LN			✓	RT		205	515
Rempe et al.[29]	304			Annealed at 1050°C for 1 h, forced-air cooled	RT 704 777	195 138 130 (See Fig. 6)	252 98 93 (See Fig. 5)	642 285 197 (See Fig. 5)
ASME Boiler and Pressure Vessel Code[30]	304, 304H, 304L, 316, 304LN, 316N, 316LN				RT to 540°C		(See Fig. 5)	(See Fig. 5)
Cheng[31] and Kang et al.[34]	304		Solution heat treated at 1150°C for 1 h		RT 200°C 400°C	233 212 194 (See Fig. 6)	338 200 144 (See Fig. 5)	
Byun et al.[32]	304, 316, 316LN			Annealed at 1050°C for 30 min after machining	RT 200°C 400°C	185 176 173 (See Fig. 6)	200 120 100 (See Fig. 5)	600 450 400 (See Fig. 5)
Engineering Toolbox[33]	304, 310, 316, 321, 347			✓	RT to 650°C	(See Fig. 6)		

[a]RT = room temperature.

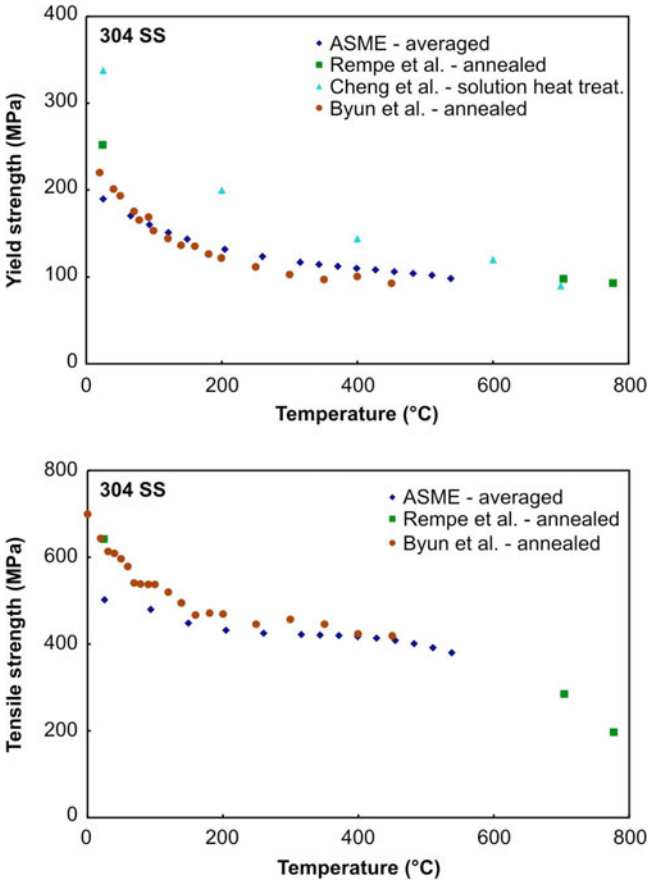

Fig. 5. Temperature dependence of the yield strength and the tensile strength of stainless steels (Type 304).

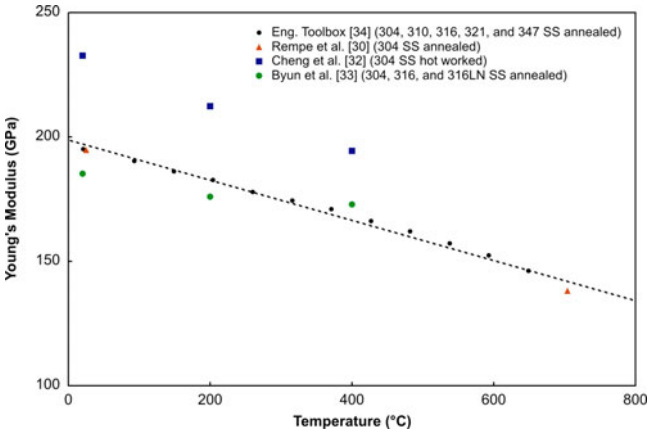

Fig. 6. Young's modulus of stainless steels as a function of temperature. See Refs. 29, 31, 32, and 33.

that material composition and testing methods also impact results.

Type 304 stainless steel is widely used in NPPs. Data suggest that at temperatures >400°C, these austenitic

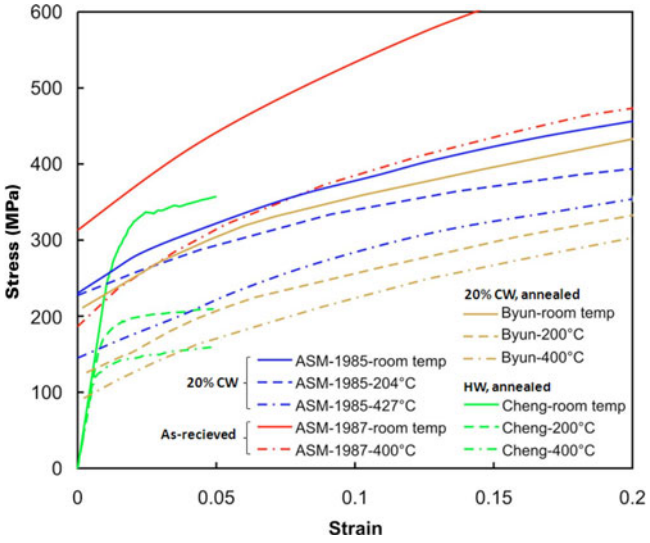

Fig. 7. Temperature dependence of engineering stress-strain curves for Type 304 stainless steel.

stainless steels have low resistance to irradiation-induced swelling and creep compared to ferritic/martensitic (F/M) steels. However, at temperatures <400°C, data suggest that Type 304 stainless steel may have much better resistance to irradiation-induced embrittlement effects than F/M steels.[7]

Although irradiation data for Type 304 stainless steel are limited, available data[32,35,36] suggest that increasing fluence accelerates the total strain. Figure 8 shows measured $\Delta D/D_o$ for Type 304 stainless steel as a function of dose in capsules irradiated in the Experimental Breeder Reactor II (EBR-II) at 390°C. Data are presented for capsules containing specimens without any load (P-19 and P-21), capsules containing specimens subjected to hoop stresses of 69 MPa (P-32, P-39, and P-49), and capsules containing specimens subjected to hoop stresses of 188 MPa (P-38 and P-48) (Refs. 7 and 35). Each specimen (tube) was 152 cm in length, with an outer diameter of 0.737 cm and 0.051-cm wall thickness. The initial diameters (D_o) were taken to be the measured D after the first irradiation cycle. The measured strains do not begin with "0" because the first irradiation cycle was not considered.[36] Curves in Fig. 8 represent irradiated data from low-dose regions (e.g., up to 17 dpa) to high-dose regions (from 17 to 89 dpa, the average of the maximum dose for all of the capsules). It is shown that in all cases, the 0 dpa intercept of the least-square fit is negative. This is simply an artifact of ignoring the irradiation strain accumulated during the first irradiation cycle (e.g., the strain does not start at zero). As shown in these figures, elongation (diametral change) is significantly increased in high-dose regions. However, traditional cook-and-look methodologies may yield less-accurate data because the measurements are not made under prototypic

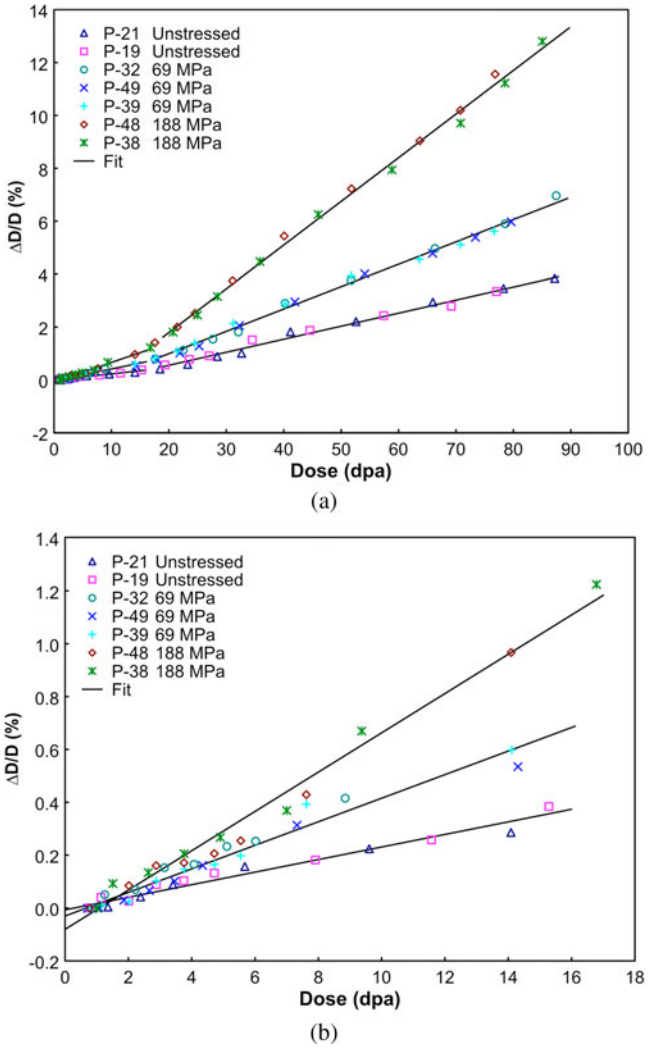

Fig. 8. Measured $\Delta D/D_o$ versus dose for the unstressed capsules (P-19, P-21), the capsules with a hoop stress of 69 MPa (P-32, P-39, P-49), and the capsules with a hoop stress of 188 MPa (P-38, P-48): (a) high dose and (b) low dose regions. The capsules were irradiated in EBR-II at a temperature of 390°C (Refs. 7 and 35).

conditions and the process of removing the sample from the reactor, making the measurements in a hot cell, and then returning the samples to the reactor may disturb results. Hence, it is desirable to obtain real-time measurements of irradiation creep under the anticipated conditions (temperature, pressure, fluence, etc.) of components in operating or advanced NPPs.

III. INL APPROACH

An instrumented creep test rig was developed to perform creep testing of specimens in PWR coolant conditions in the ATR. A prototype creep test rig was first tested in an autoclave at INL's HTTL to evaluate the performance of this design. Results from autoclave evaluations were used to finalize a test rig design for use in an ATR PWR loop. This section provides a summary description of the test rig design, the autoclave evaluation approach, and representative results. More detailed information may be found in Refs. 9 and 19.

III.A. Design

Figure 9 identifies major components of the INL prototype test rig and positioning standoffs for autoclave testing. Similar to the test rigs discussed in Sec. II, major components in the INL test rig include a tensile specimen, a bellows, an LVDT, and fixturing to connect these components. The IFE/HRP provided the LVDT and welded the LVDT, bellows, and connecting fixturing in this test rig using electron-beam and seal welding techniques. Figure 10 shows the test rig inserted in the autoclave.

III.B. Autoclave Setup

Figure 11 shows the autoclave and supporting equipment layout for prototype creep test rig evaluations. The autoclave was designed for operation at a maximum allowable working pressure of 22.8 MPa. A pressure relief valve, currently set at 19.3 MPa, prevents overpressurization of the autoclave. The heater is controlled by a proportional-integral-derivative controller, which uses the

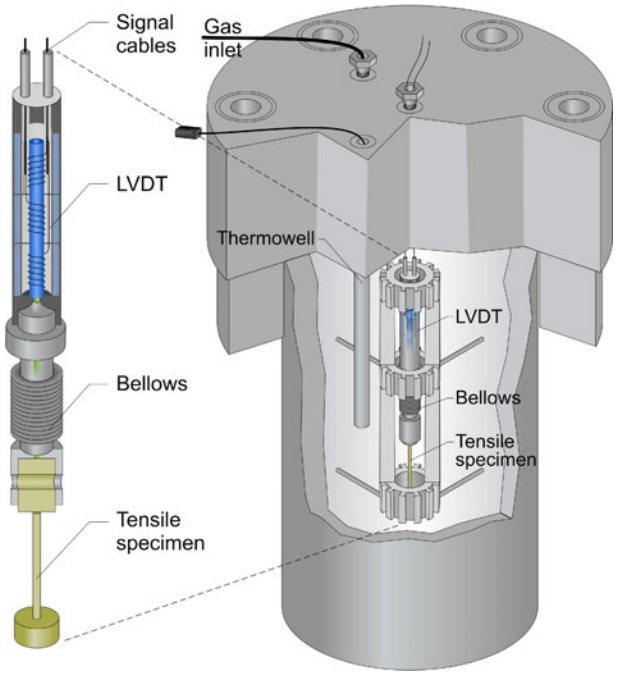

Fig. 9. Schematic of test rig positioned in autoclave for testing.

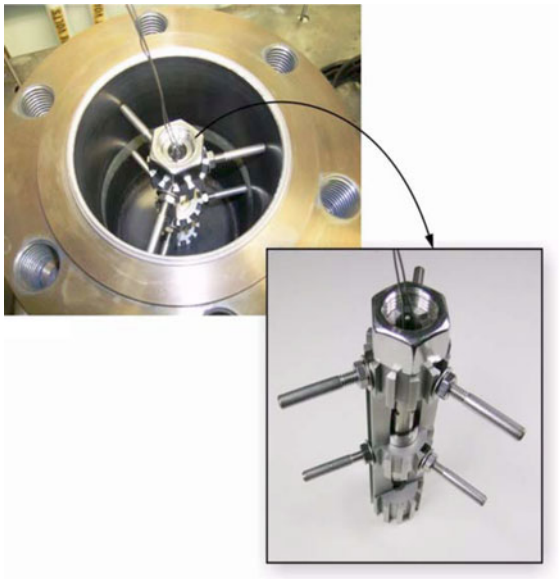

Fig. 10. Test rig inserted into fixture with autoclave-positioning structures.

thermocouple inserted into the thermowell to detect and control temperature. An overtemperature thermocouple, which is located between the heater and the vessel body, shuts off the heater if the vessel temperature exceeds the user-specified high-temperature limit. The subcooled water pressure is maintained by the high-pressure pump, which will run throughout each experiment. The system pressure is controlled by the backpressure regulator, which is manually set for the specific experiment. The vent valve is used to manually vent the air as the system fills and also to vent air that is released from solution as the water is heated. Instrument leads from the test rig exit the autoclave through an appropriately configured Conax fitting. A data acquisition system records data from the LVDT, the temperature from a second thermocouple inserted into the thermowell, and the pressure from the pressure transducer installed in the system tubing. Proposed coolant conditions for autoclave testing at the ATR PWR loop conditions are listed in Table III.

III.C. Tensile Specimen Selection

Tensile specimen size was selected based on anticipated loads during creep testing at PWR pressures. In addition, specimen geometry was influenced by the need to minimize size during irradiation testing and the need to obtain elongations that can be detected by the LVDT. Using Eqs. (5), (6), and (7), the force that will be exerted on the specimen, F_{spec}, is estimated by subtracting the force required to compress the bellows, $F_{bellows}$, from the total force applied to the bellows, F_{total}:

$$F_{spec} = F_{total} - F_{bellows} \ , \tag{5}$$

$$F_{bellows} = SR \cdot d \ , \tag{6}$$

TABLE III

Experimental Parameters for Autoclave Coolant

Coolant	Pressurized H_2O
Temperature (°C)	280 to 350
System pressure (MPa)	15.5 to 15.9
Coolant pH (at 25°C)	4.2 to 10.5

and

$$F_{total} = P_{system} \cdot (A_{ext\text{-}eff} - A_{specimen}) \ , \tag{7}$$

where

SR = bellows spring rate [N/m (lb_f/in.)]

d = sample elongation [m (in.)]

$A_{ext\text{-}eff}$ = bellows external effective area [m^2 ($in.^2$)]

$A_{specimen}$ = area of the test section of specimen [m^2 ($in.^2$)]

P_{system} = system pressure [N/m^2 ($lb_f/in.^2$)].

For the bellows SR (e.g., 3514 N/m) and the anticipated maximum sample elongation in these creep tests, d (e.g., 25.4×10^{-9} m), the force to compress the bellows is negligible compared to the total force applied to the bellows at system pressure (e.g., $F_{bellows} \ll F_{total}$). Using the effective external bellows area (0.84 cm^2), the specimen test area, and a representative PWR pressure (15.5 MPa), the peak force exerted on the specimen is 1300 N. Applying Eq. (8), an appropriate specimen radius r_{spec} can be selected to obtain the desired range of stresses (90 to 350 MPa) for this PWR pressure:

$$\sigma_{spec} = \frac{F_{spec}}{\pi r_{spec}^2} \ . \tag{8}$$

Ultimately, the test rig will be used to evaluate several types of specimen materials, including Type 304 stainless steel, INCONEL® alloy 600,[a] and Type 316 stainless steel. However, initial checkout focused on Type 304 stainless steel and copper specimens. As noted above, elongation measurements were initially compared with data presented in Sec. II and with data obtained from INL load frames for samples that come from the same batch of material with similar fabrication and heat treatment processes. Ultimately, elongation measurements were compared with posttest measurements made with a micrometer.

[a]INCONEL is a registered trademark of the Special Metals Corporation group of companies.

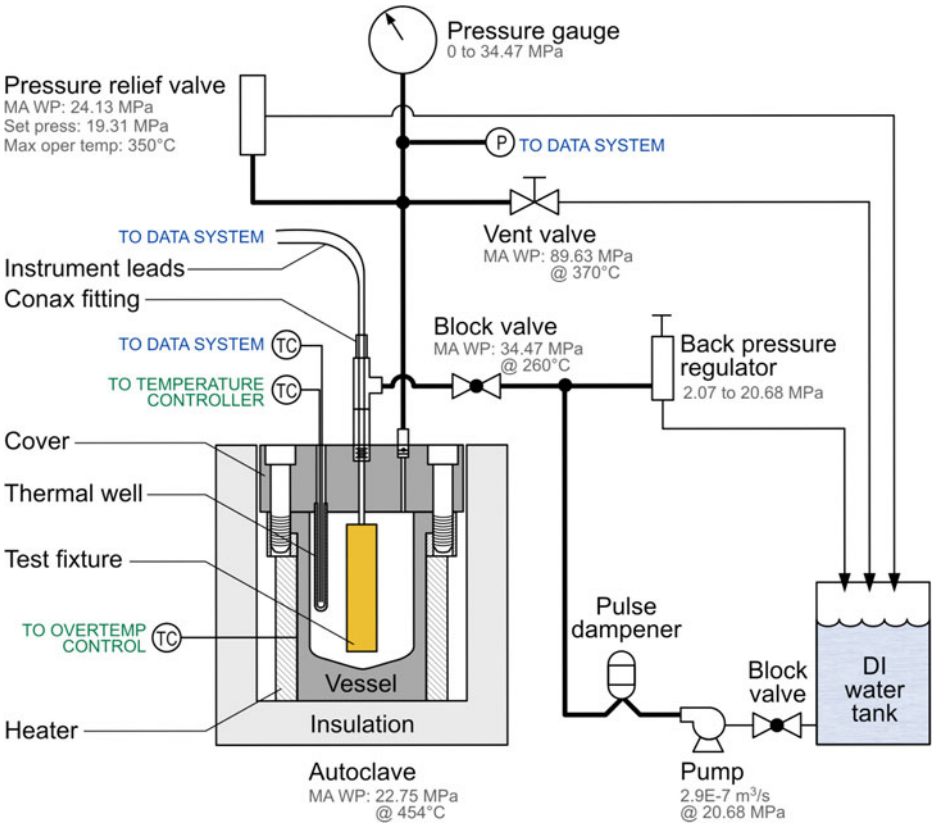

Fig. 11. Autoclave and supporting equipment layout.

IV. INITIAL AUTOCLAVE RESULTS

IV.A. Test Objectives

Objectives for the autoclave evaluations of the prototype test rig included the following:

1. check out test rig design and verify that it can withstand PWR coolant temperatures and pressures
2. verify operation of signal processing equipment
3. calibrate test rig design using samples with known creep behavior
4. obtain insights for an enhanced creep test rig design that will be inserted into an ATR PWR loop.

IV.B. Checkout Tests

To address the first two objectives, a Type 304 stainless steel specimen, with a gauge diameter of 2 mm and a gauge length of 28 mm, was loaded into the creep test rig; and the entire assembly was placed inside the autoclave. Instrument indications for temperature, pressure, and the LVDT output voltage were noted while the autoclave temperature and pressure remained at normal conditions. All indications were consistent with the autoclave conditions. The autoclave temperature and pressure were then gradually increased and ultimately stabilized at ~300°C and ~15.5 MPa. The corresponding instrument indications for temperature, pressure, and the LVDT output voltage were again noted. Those indications were also consistent with the autoclave conditions. Furthermore, changes in the instrument indications, relative to readings under normal conditions, were reasonable. Finally, the autoclave temperature and pressure were allowed to return to normal conditions. When the system stabilized, instrument indications returned to those consistent with normal conditions.

This sequence provided indications that the creep test rig functioned as designed and that the creep test rig can withstand the PWR coolant conditions. In addition, instrument indications for temperature, pressure, and the LVDT output voltage indicated that signal processing equipment operated properly. It should be noted that simple observations, like those just described, were made during the course of completing all autoclave testing. Those observations confirmed satisfactory performance of the creep test rig and associated instrumentation relative to the first two objectives.

IV.C. Testing

Although evaluation of creep behavior is the primary design goal for this fixture, testing in the elastic region was initially pursued to assess the performance of the test rig design. Room temperature measurements were made using two Type 304 stainless steel specimens (with a gauge diameter of 2 mm and a gauge length of 28 mm). Limiting the stress to a level below the yield strength was initially pursued because it ensured that the sample remained intact, precluding concerns regarding possible adverse affects on the creep test rig that might accompany specimen failure. However, data obtained from such tests were inconclusive because of accuracy limitations associated with this method.

Evaluations were then conducted in which copper (Cu) and Type 304 stainless steel specimens were loaded beyond their yield strengths as a result of elevated autoclave pressures and temperatures. These evaluations were of interest because specimen deformations beyond elastic limits should be much larger than any deformations that may develop in the creep test rig itself. As a result, these evaluations provided an understanding of the LVDT response relative to the actual specimen elongation while minimizing any complications introduced by small deformations of the creep test rig. A (nominal) gauge diameter of 2 mm and a (nominal) gauge length of 28 mm were adopted for all specimens in these tests.

In each test, specimen measurements based on the LVDT outputs were compared with micrometer measurements. These comparisons were limited to measurements at the end of each test because micrometer measurements were impossible while the autoclave was pressurized. Although comparisons were limited to the "end state" for each specimen, the comparisons were used to indicate whether specimen elongations can be correctly detected and recorded using the creep test rig. A summary of results for all tests conducted in the plastic region is provided in Table IV. As indicated in Table IV, Cu and Type 304 stainless steel (304SS) specimens were tested at elevated pressures at room temperature and at elevated temperatures. In all cases, disparities between the LVDT and micrometer measurements with respect to final lengths were found to be very small (<0.9%). These disparities correspond with errors in length of 0.26 mm or less, which is considered to be close agreement given the measurement techniques that were used.

V. SUMMARY AND CONCLUSION

As part of the ATR NSUF, an instrumented creep testing capability was developed to allow specimens to be tested during irradiation in PWR coolant conditions, e.g., applied loads up to 350 MPa at temperatures up to 370°C. Results from laboratory evaluations of a prototype creep test rig were incorporated into a final design that will be inserted into the ATR PWR loop.

As noted in this paper, there are other international research efforts to develop in-pile creep testing capabilities at MTRs. In-pile creep tests that can provide real-time data for detecting specimen elongation and controlling loads applied to the specimens have already been completed in these international research efforts. However, the setup evaluated in the BR2 in Belgium was the only setup capable of testing samples subjected to prototypic LWR coolant temperatures and pressures.

Although the INL-developed creep testing capability will ultimately be used for a wide range of materials, initial efforts focused on Type 304 stainless steel. Existing tensile and creep data for unirradiated and irradiated

TABLE IV

Results from Testing in the Plastic Region

Specimen[a]	Description	Final Length (mm)		Length Disparity	
		LVDT	Micrometer	(mm)	(%)
SSX	304SS-x, to 19.9 MPa at room temperature	29.16	29.25	−0.09	0.31
SS01	304SS-1, to 19.3 MPa at room temperature	29.85	30.05	−0.02	0.65
SS02	304SS-2, to 19.1 MPa at room temperature	29.67	29.85	−0.18	0.61
SS03	304SS-3, to 16.3 MPa with a peak of 245°C	29.90	29.95	−0.05	0.17
SS04	304SS-4, to 15.9 MPa with a peak of 156°C	29.83	29.93	−0.10	0.33
Cu01	Cu-1, to 11.9 MPa at room temperature	30.32	30.36	−0.04	0.13
Cu02	Cu-2, to 11.9 MPa at room temperature	30.21	30.32	−0.11	0.36
Cu03	Cu-3, to 11.1 MPa with a peak of 170°C	28.98	29.24	−0.26	0.09
Cu04	Cu-4, to 12.6 MPa with a peak of 200°C	28.55	28.64	−0.09	0.31

[a]After machining, all stainless steel specimens, except SSX, were annealed in Ar at 1050°C for 30 min then cooled in air. After machining, all Cu specimens were annealed at 650°C for 35 min then quenched in water.

stainless steels (Type 304) were reviewed to gain insights about the impact of temperature and radiation on the structural properties of this material. Existing data for irradiated materials illustrate that the strength of Type 304 stainless steel degrades during irradiation, especially at high temperatures. Irradiation data indicate that at temperatures >400°C and/or at high doses up to a maximum dose of 93.3 dpa, austenitic stainless steels (Type 304) have low resistance to irradiation-induced swelling and creep. However, at lower temperatures, Type 304 stainless steels may have much better resistance to irradiation-induced embrittlement effects as compared to F/M steels.

Laboratory evaluations of an INL-developed prototype creep test rig in an autoclave testing system were completed. Major components of this creep test rig include a tensile specimen, a bellows, an LVDT, and fixturing to connect these components. The initial performance of this test rig was assessed using pressurization tests for a 2-mm gauge diameter, 28-mm gauge length, Type 304 stainless steel specimen. Results indicate that the signal processing equipment did perform as anticipated. Although evaluation of creep behavior is the primary design goal for this fixture, testing in the elastic region was initially pursued to assess the performance of the test rig design. However, data obtained from such tests were inconclusive because of accuracy limitations associated with this method.

Evaluations were then conducted in which copper (Cu) and Type 304 stainless steel specimens were loaded beyond their yield strengths as a result of elevated autoclave pressures and temperatures. In each test, specimen measurements based on the LVDT output were compared with micrometer measurements. Disparities between the LVDT and micrometer measurements with respect to final lengths were found to be very small (<0.9%). These disparities correspond to errors in length of 0.26 mm or less. Hence, the LVDT data were in close agreement with micrometer data given the measurement techniques that were used.

In summary, testing of the prototype test rig confirmed the viability of the proposed design. Only minor modifications were incorporated into a revised design that is planned to be deployed in an ATR PWR loop in 2012.

ACKNOWLEDGMENTS

This work was supported by the U.S. Department of Energy, Office of Nuclear Energy, Science, and Technology, under DOE-NE Idaho Operations Office Contract DE AC07 05ID14517. The authors would also like to express their appreciation to the National Research Foundation grant funded by the Ministry of Education, Science and Technology of the Republic of Korea for the support of B. G. Kim through the project for National Nuclear R&D Program. In addition, the authors would like to express special thanks to S. Solstad, IFE/HRP, for his assistance and comments.

REFERENCES

1. D. L. PORTER, G. D. HUDMAN, and F. A. GARNER, "Irradiation Creep and Swelling of Annealed Type 304 Stainless Steel at ~390°C and High Neutron Fluence," *J. Nucl. Mater.*, **179–181**, 581 (1991).

2. W. SCHÜLE and H. HAUSEN, "Neutron Irradiation Creep in Stainless Steel Alloys," *J. Nucl. Mater.*, **212–215**, 388 (1994).

3. J. NAKAGAWA, "Calculation of Radiation-Induced Creep and Stress Relaxation," *J. Nucl. Mater.*, **225**, 1 (1995).

4. F. A. GARNER, M. B. TOLOCZKO, and M. L. GROSSBECK, "The Dependence of Irradiation Creep in Austenitic Alloys on Displacement Rate and Helium to dpa Ratio," *J. Nucl. Mater.*, **258–263**, 1718 (1998).

5. J. P. FOSTER, K. BUNDE, M. L. GROSSBECK, and E. R. GILBERT, "Temperature Dependence of the 20% Cold Worked 310 Stainless Steel Steady State Irradiation Creep Rate," *J. Nucl. Mater.*, **270**, 357 (1999).

6. Y. KURATA et al., "In-Pile and Post-Irradiation Creep of Type 304 Stainless Steel Under Different Neutron Spectra," *J. Nucl. Mater.*, **283–287**, 386 (2000).

7. J. P. FOSTER, K. BUNDE, and D. L. PORTER, "Irradiation Creep of Annealed 304L Stainless Steel at Low Dose Levels," *J. Nucl. Mater.*, **317**, 167 (2003).

8. T. R. ALLEN and J. T. BUSBY, "Radiation Damage Concerns for Extended Light Water Reactor Service," *J. Min. Met. Mater. Soc.*, **61**, *7*, 29 (2009).

9. B. G. KIM, J. L. REMPE, D. L. KNUDSON, K. G. CONDIE, and B. H. SENCER, "In-Situ Creep Testing Capability Development for the Advanced Test Reactor," INL/EXT-10-17779, Idaho National Laboratory (Apr. 2010).

10. P. MOILANEN, S. TÄHTINEN, B. N. SINGH, and P. JACQUET, "In-Situ Investigation of the Mechanical Performance and Life Time of Copper: Final Report on Design, Construction, and Calibration of Test Module for In-Reactor Tensile Tests in BR-2 Reactor," BTUO 76-031127, VTT (Oct. 27, 2004).

11. N. SINGH, S. TÄHTINEN, P. MOILANEN, P. JACQUET, and J. DEKEYSER, "In-Reactor Uniaxial Tensile Testing of Pure Copper at a Constant Strain Rate at 90°C," *J. Nucl. Mater.*, **320**, 299 (2003).

12. R. VAN NIEUWENHOVE and S. SOLSTAD, "In-Core Fuel Performance and Material Characterization in the Halden Reactor," ANIMMA Int. Conf., Marseille, France, June 7–10, 2009.

13. S. SOLSTAD and R. VAN NIEUWENHOVE, "Instrument Capabilities and Developments at the Halden Reactor Project," *Proc. Sixth Int. Topl. Mtg. Nuclear Plant Instrumentation, Control, and Human-Machine Interface Technologies (NPIC&HMIT 2009)*, Knoxville, Tennessee, April 5–9, 2009, American Nuclear Society (2009) (CD-ROM).

14. W. WIESENACK, "Status and Outlook for Irradiation Testing ... from a Halden Reactor Perspective ... Mostly," Presented at *Int. Conf. Physics of Reactors: Nuclear Power: A Sustainable Resource*, Interlaken, Switzerland, September 14–19, 2008; see also W. WIESENACK and T. TVERBERG, "The OECD Halden Reactor Project Fuels Testing Programme: Methods, Selected Results and Plans," *Nucl. Eng. Des.*, **207**, 189 (2001).

15. T. M. KARLSEN, "Achievements and Further Plans for the OECD Halden Reactor Project Materials Programme," *Nucl. Eng. Des.*, **207**, 199 (2001).

16. J.-F. VILLARD, "State-of-the-Art and Improvement of Online Measurements in Present and Future French Research Reactors," presentation at Idaho National Laboratory (Sep. 2009).

17. P. BENNETT and T. KARLSEN, "In-Core Corrosion Monitoring in the Halden Test Reactor," *Energy Mater.*, **3**, *2*, 81 (June 2008).

18. F. ØWRE and M. McGRATH, "Present Status and Future Plans of the Halden Reactor," presented at 12th IGORR, Beijing, China, October 28–31, 2009.

19. D. L. KNUDSON and J. L. REMPE, "Linear Variable Differential Transformer (LVDT)-Based Elongation Measurements in Advanced Test Reactor High Temperature Irradiation Testing," *Meas. Sci. Technol.*, **23**, *2* (February 2012).

20. L. E. REHN, "Production of Freely-Migrating Defects," *J. Nucl. Mater.*, **174**, 144 (1990).

21. H. HAUSEN and W. SCHÜLE, "Neutron Irradiation Creep at 100°C on 316L AMCR, Welded 316L Stainless Steel Alloys," *Proc. 18th Int. Symp. Effects of Radiation on Materials*, Hyannis, Massachusetts, June 25–27, 1996, ASTP STP 1325, pp. 830–849.

22. B. G. KIM et al., "Status and Perspective of Material Irradiation Tests in the HANARO," presented at 1st Int. Symp. Materials Testing Reactors, Oarai, Japan, July 2008.

23. B. G. KIM, K.-N. CHOO, J. M. SOHN, S. J. PARK, Y. K. KIM, and Y. J. KIM, "Instrumentations for Materials Irradiation Tests in HANARO," *Proc. Topl. Mtg. Nuclear Plant Instrumentation, Controls, and Human Machine Interface Technology (NPIC HMIT 2009)*, Knoxville, Tennessee, April 2009, American Nuclear Society (2009).

24. B. G. KIM, K. N. CHOO, Y. K. KIM, and J. J. HA, "Irradiation and Instrumentation Technology in HANARO," presented at 2nd Int. Symp. Material Test Reactors, Idaho Falls, Idaho, September 28–October 1, 2009.

25. B. G. KIM, J. M. SOHN, and K. N. CHOO, "Development Status of Irradiation Devices and Instrumentation for Material and Nuclear Fuel Irradiation Tests in HANARO," *Nucl. Eng. Technol.*, **42**, *2*, 203 (Apr. 2010).

26. "Appendices," Sec. 9 of *Specialty Steels Product Reference Manual*, Atlas Steels Web site: http://www.atlassteels.com.au/documents/Stainless%20Steel%20Grade%20Composition%20Chart.pdf (current as of Apr. 1, 2010).

27. Y. S. TOULOUKIAN, R. K. KIRBY, R. E. TAYLOR, and P. D. DESAI, *Thermophysical Properties of Matter*, Vol. 12, *Thermal Expansion Metallic Elements and Alloys*, Figure and Table 258R, "Provisional Values for Thermal Linear Expansion of Iron + Chromium + ΣXi Alloys," IFI/Plenum, New York (1975).

28. *Atlas of Stress-Strain Curves*, H. E. BOYER, Ed., p. 294, ASM International, Metals Park, Ohio (1987); see also *Metals Handbook*, Vol. 3, *Properties and Selection: Stainless Steels, Tool Materials, and Special-Purpose Metals*, 9th ed., p. 35, American Society for Metals, Metals Park, Ohio (1985).

29. J. L. REMPE et al., "Light Water Reactor Lower Head Failure Analysis," NUREG/CR-5642, EGG-2618, Idaho National Engineering Laboratory (Oct. 1993).

30. *ASME Boiler & Pressure Vessel Code*, Sec. II, Part D, "(Customary) Materials," 2007 Ed., pp. 517–524 and 642–654, American Society of Mechanical Engineers (July 1, 2007).

31. P.-Y. CHENG, "Influence of Residual Stress and Heat Affected Zone on Fatigue; Failure of Welded Piping Joints," PhD Thesis, North Carolina State University, Raleigh (2009).

32. T. S. BYUN, N. HASHIMOTO, and K. FARRELL, "Temperature Dependence of Strain Hardening and Plastic Instability Behaviors in Austenitic Stainless Steels," *Acta Mater.*, **52**, 3889 (2004).

33. "Young Modulus of Elasticity for Metals and Alloys," Engineering ToolBox Web site: http://www.engineeringtoolbox.com/young-modulus-d_773.html (current as of April 1, 2010).

34. G. Z. KANG, Y. G. LI, and Q. GAO, "Non-Proportionally Multiaxial Ratcheting of Cyclic Hardening Materials at Elevated Temperatures: Experiments and Simulations," *Mech. Mater.*, **37**, 1101 (2005).

35. D. L. PORTER and G. D. HUDMAN, "Irradiation Creep and Swelling of Annealed Type 304L Stainless steel at −390°C and High Neutron Fluence," *J. Nucl. Mater.*, **179–181**, 581 (1991).

36. G. L. McVAY, L.C. WALTERS, and G. D. HUDMAN, "Neutron Irradiation-Induced Creep of Helium Pressurized 304L Stainless Steel Capsules," *J. Nucl. Mater.*, **79**, 395 (1979).

37. J. REMPE, D. KNUDSON, J. DAW, T. UNRUH, B. CHASE, and K. DAVIS, "Enhanced In-Pile Instrumentation at the Advanced Test Reactor," *IEEE Trans. Nucl. Sci.*, IEEE (2011).